In Vitro Cellular & Developmental Biology - Animal (2020) 56:604–613
https://doi.org/10.1007/s11626-020-00497-8

Discriminating aspects of global metabolism of neonatal cardiomyocytes from wild type and KO-CSRP3 rats using proton magnetic resonance spectroscopy of culture media samples

Antonio Carlos Bloise[1] · Jennifer Adriane dos Santos[1,2] · Isis Vasconcelos de Brito[1] · Vinicius Bassaneze[2] · Ligia Ferreira Gomes[1,3] · Adriano Mesquita Alencar[1]

Received: 30 April 2020 / Accepted: 10 August 2020 / Published online: 10 September 2020 / Editor: Tetsuji Okamoto

Abstract

Knockout of multifunction gene cysteine- and glycine-rich protein 3 (CSRP3) in cardiomyocytes (CMs) of mice leads to heart dilation, severely affecting its functions. In humans, CSRP3 mutations are associated with hypertrophic (HCM) and dilated cardiomyopathy (DCM). The absence of the CSRP3 expression produces unknown effects on in vitro neonatal CMs' metabolism. The metabolome changes in culture media conditioned by CSRP3 knockout (KO-CSRP3), and wild type (WT) neonatal cardiomyocytes were investigated under untreated or after metabolic challenging conditions produced by isoproterenol (ISO) stimulation, by in vitro high-resolution proton magnetic resonance spectroscopy (^{1}H-MRS)-based metabolomics. Metabolic differences between neonatal KO-CSRP3 and WT rats' CMs were identified. After 72 h of culture, ISO administration was associated with increased CMs' energy requirements and increased levels of threonine, alanine, and 3-hydroxybutyrate in both neonatal KO-CSRP3 and WT CMs conditioned media. When compared with KO-CSRP3, culture media derived from WT cells presented higher lactate concentrations either under basal or ISO-stimulated conditions. The higher activity of ketogenic biochemical pathways met the elevated energy requirements of the contractile cells. Both cells are considered phenotypically indistinguishable in the neonatal period of animal lives, but the observed metabolic stress responses of KO-CSRP3 and WT CMs to ISO were different. KO-CSRP3 CMs produced less lactate than WT CMs in both basal and stimulated conditions. Mainly, ISO-stimulated conditions produced evidence for lactate overload within KO-CSRP3 CMs, while WT CMs succeeded to manage the metabolic stress. Thus, ^{1}H-MRS-based metabolomics was suitable to identify early inefficient energetic metabolism in neonatal KO-CSRP3 CMs. These results may reflect an apparent lower lactate transport and consumption, in association with protein catabolism.

Keywords Cardiomyocytes · Cysteine- and glycine-rich protein 3 · Knockout animal · Proton magnetic resonance spectroscopy · Metabolomics

Introduction

Cardiomyocytes (CMs) are the cells that constitute the contractile portion of cardiac tissue (Zhang *et al.* 2008), combining electrophysiological, biochemical, and mechanical functions (Martínez *et al.* 2017). The study of CMs' metabolism addresses the maintenance of these functions and how the implied molecular pathways affect energy consumption. Proton magnetic resonance spectroscopy (^{1}H-MRS)-based metabolomics is a multiscale methodological approach (Griffin and Shockcor 2004; J C Lindon *et al.* 2006; Kaddurah-Daouk *et al.* 2008; Finckenberg and Mervaala 2010; Nicholson 2010; Bacchi *et al.* 2014; Saborano *et al.* 2019). It can be applied to measure the global metabolism of CMs and allows further associations with their in vivo

Electronic supplementary material The online version of this article (https://doi.org/10.1007/s11626-020-00497-8) contains supplementary material, which is available to authorized users.

✉ Antonio Carlos Bloise
acbloise@if.usp.br

[1] Laboratory of Microrheology and Molecular physiology, Instituto de Física, Universidade de São Paulo, São Paulo 05508-090, Brazil

[2] Laboratory of Genetics and Molecular Cardiology/LIM 13, Heart Institute (InCor), University of São Paulo Medical School, São Paulo 05403-000, Brazil

[3] Faculty of Pharmaceutical Sciences, University of São Paulo, São Paulo 05508-000, Brazil

behavior (Mandenius *et al.* 2011). This approach enables the study of the metabolic status of normal and genetically modified CMs in basal conditions or under pharmacological influences (Chaudhari *et al.* 2017). Metabolomics was employed to describe very early stage anomalies of hypertrophic cardiomyopathy (HC) in CMs from a genetically modified neonatal rat model. Most of the HCs result from sarcomeric gene mutations. It is known that the sarcomere is the fundamental contractile unit within the CMs, and cysteine- and glycine-rich protein 3 (Csrp3) has diverse functional roles including transcriptional regulation, signal transduction, cytoskeletal organization, and glucose homeostasis (Ehsan *et al.* 2018; Hernandez-Carretero *et al.* 2018). The importance of CSRP3 on heart function was previously demonstrated by experimental evidence. In CSRP3 knocked out (KO) mice, the cardiac phenotype is similar to dilated cardiomyopathy (Arber *et al.* 1997). In humans, CSRP3 mutations are directly associated with familial HC (Geier *et al.* 2003). At the subcellular level, Csrp3 protein can be detected in the cytoplasm (Boateng *et al.* 2009) and nucleus (Geier *et al.* 2003). As documented by clinical, experimental, and molecular reports, Csrp3 acts as a signaling element, responsive to pharmacological or mechanical stimuli, and α-actinin and myogenin are among its several binding partners (Lange *et al.* 2016). Pharmacological treatment with a beta-adrenoceptor agonist, such as isoproterenol (ISO) accelerates the HC manifestation (Li *et al.* 2019). The neonatal KO-CSRP3 CMs are phenotypically indistinguishable of the neonatal wild type cells. However, the metabolic effects of ISO in neonatal CSRP3 knockout (KO-CSRP3) CMs are still unknown.

It was hypothesized that ISO action could increase Csrp3 biochemical fingerprints in neonatal cardiomyocytes' metabolic profile. A study was designed to evaluate whether ^{1}H-MRS-based metabolomics could demonstrate the Csrp3 deficiency in KO-CSRP3 rats' CMs' metabolism either at the basal condition or under ISO stimulation. The conditioned culture media from non-proliferative CMs' cultures were used as the magnetic resonance samples in the characterization of the metabolic differences between WT and KO-CSRP3 cells. Potential extracellular biomarkers detected by ^{1}H-MRS were investigated to describe premature differences between wild type (WT) and KO-CSRP3 CMs. This approach was reproducible and exhibit a short acquisition time, eliminating the need for any additional chemical separation process. Considering that heartbeat functional overload triggers and sustain a defective phenotype in adult cells (R. Li *et al.* 2013), a 24-h isoproterenol (ISO) challenge was applied to increase the in vitro beating frequency of neonatal KO-CSRP3 CMs. Then, metabolomic analysis of the culture medium was conducted to disclose the impact of the genetic alterations upon metabolism. The strategy of early inducing metabolic differences between lineages can help to improve the evaluation of drug-induced cardiotoxicity.

Materials and Methods

Cell culture and sample preparation Primary neonatal CMs were obtained from WT and knockout CSRP3 (KO-CSRP3) rats, as previously described elsewhere (Jensen *et al.* 2018). Cells were pooled from 10 to 15 neonatal hearts from each lineage and frozen in liquid nitrogen. The distinct cell samples were prepared as isolated and purified lineage cells during the extraction step (up to 85% after 72 h of culture), and a DNA test using Proteinase K Method confirmed the CMs' isolation (Campos *et al.* 2018). All the experimental procedures were performed according to the guidelines for ethical conduct used in animal care and approved by the local institutional review board: University of Sao Paulo Medical School, Brazil (#340/12). Cells were thawed and seeded into four 24-well plates (256 ± 61 thousand cells per well) previously recovered with laminin (1 μg/mL in PBS per well; 37°C for 2-h incubation). The development of non-cardiomyocyte cells was prevented by incubation with a 4:1 proportion mixture of DMEM (Dulbecco's Modified Eagle Medium low glucose, Gibco®, Waltham, MA): M199 (Media 199, Gibco®) culture media supplemented with 1% (v/v) of horse serum (HRS, Gibco®), 5% of newborn calf serum (NBCS, Gibco®), and 1% of bromodeoxyuridine (BrdU, Gibco®). Cells were incubated for 48 h in a commercial CO_2 incubator (Series II Water Jacket, Thermo Scientific, Waltham, MA), and spontaneous cell pulse was observable, confirming the purity of cell culture. The wells were then washed twice with phosphate buffer saline (PBS, Sigma-Aldrich®, St. Louis, MO) to remove the non-viable cells. The remaining adherent WT and KO-CSRP3 cells were incubated for 24 h more, with 1 mL fresh media. Then, 2 μL of ISO solution (5 mM, diluted in deionized water) or deionized water was added to the wells, to produce the ISO-stimulated metabolic state samples and the corresponding untreated control samples (basal condition). The negative controls were produced from culture medium incubated in cell-free, laminin-coated wells. The culture media were harvested after 24 h. The span of incubation was determined to be long enough to disclose the differences in global metabolism and short enough to avoid the interference of media component deprivation or doxorubicin-induced cellular death which could mask the primary metabolic effects of the mutation. After the experimental procedures, the total volume of each well containing the media and the non-adhered CMs was transferred to 15 mL tubes and centrifuged for 10 min at ~ 1400*g*. The corresponding supernatants (~ 850 μL) were transferred to lyophilization vials, frozen at − 80°C, and lyophilized within 24 h. The lyophilized extracts were diluted in 650 μL of deuterium oxide (D_2O, Sigma-Aldrich®) containing 4,4-dimethyl-4-silapentane-1-sulfonic acid (DSS, Sigma-Aldrich®) at 0.5 mM and finally moved into 5-mm resonance tubes, immediately before the resonance experiments. In this step, the remaining viable cells were used for DNA isolation

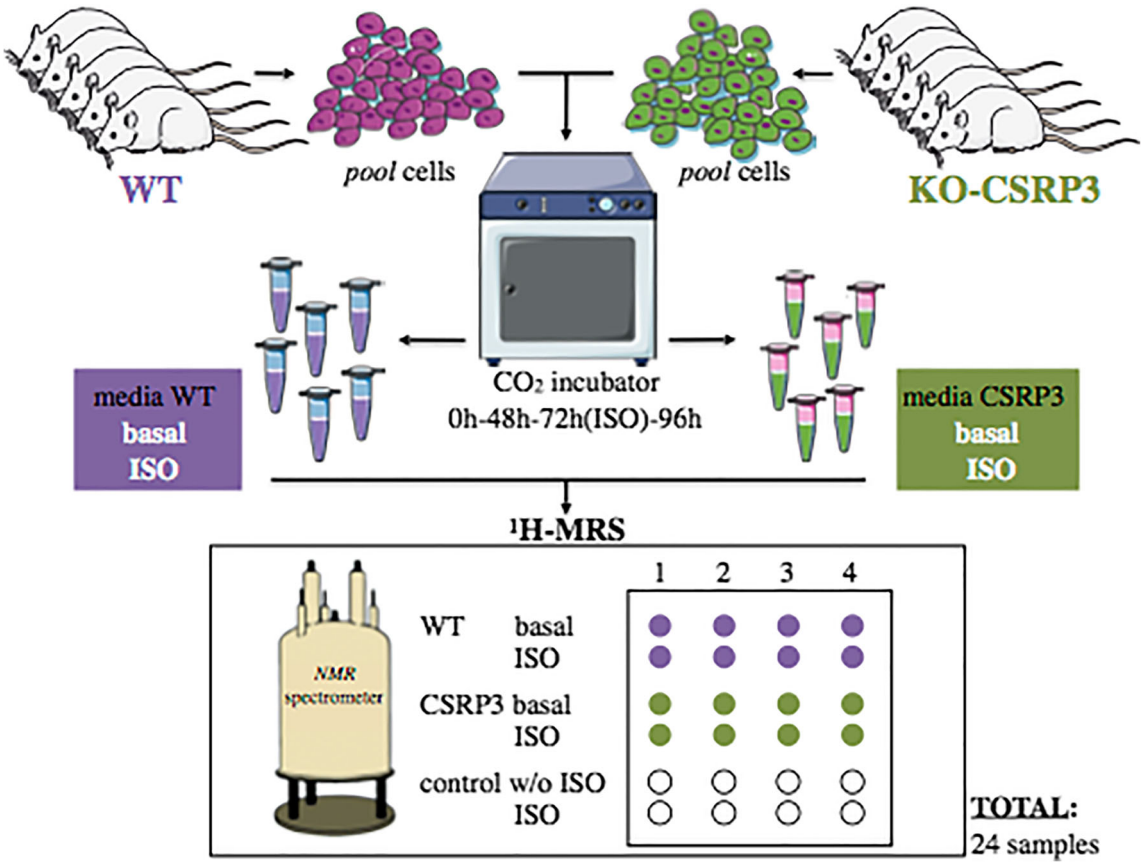

Figure 1. Culture media conditioning strategy: primary CMs obtained from WT or KO-CSRP3 neonate rats were seeded into 24-well plates, previously coated with laminin. For cell culture, a 4:1 DMEM:M199 culture medium was used, supplemented with 1% (v/v) horse serum (HRS), 5% newborn calf serum (NBCS), and 1% bromodeoxyuridine (BrdU). After 48 h of incubation, the media were removed and cells washed with PBS. Then, fresh media (1 ml) was added in each well and a new round of 24-h incubation was performed. Afterward, half wells were added with ISO (panel ^{1}H-MRS) and incubated for 24 h. Finally, after 96 h, all media samples were analyzed by NMR. Data points were processed in quadruplicates, and the culture media of equivalent quadruplicates were analyzed independently. The whole assay was performed four times ($n = 4$). Figure adapted from "Servier Medical ART," a repository of free medical images provided by Les Laboratoires Servier (http://smart.servier.com) and licensed under a Creative Commons Attribution 3.0 Unported License.

tests to confirm lineage identities. Figure 1 summarizes the whole process, including the cell conditioning strategy, media sampling for the resonance experiments, as well as the adopted classification for the experimental groups. The complete assay was repeated four times ($n = 4$), one for each plate.

Proton magnetic resonance spectroscopy Biochemical transformations in WT and KO-CSRP3 CMs were identified in ^{1}H resonance spectra of 24 independent culture media samples. Samples were divided into six groups, containing 4 sets with identical characteristics (biological replicates) each. Classification and labeling were done with a two-letter code: one standing for basal ("b") or ISO-stimulated ("i") condition and the other indicating if the culture medium was obtained from WT neonate rats ("w" at basal or "W" for ISO-stimulated) or KO-CSRP3 neonate rats ("k" or "K," basal and ISO-stimulated, respectively). The negative controls were coded as "c" or "iC" if corresponding to culture media without or with isoproterenol, respectively.

To minimize biological variations, all the cells for each experimental group testing were collected, pooled, and frozen in liquid nitrogen on the same day, from the same group of rats. After incubation, the culture medium was immediately collected and frozen in an ultra-freezer for posterior analysis. The entire procedure was validated by MVA, grouping samples according to the day of experiments instead of biological replicates to investigate the extent of systematically occurring changes in the levels of metabolites (results summarized in Supplementary Figure S1, complemented by Supplementary Figures S2 and S3, of Supplementary Materials). The ^{1}H-MRS experiments were performed at 25°C on a Varian/Agilent Inova equipment (Varian Associates, Inc., Palo Alto, California), with four channels and pulsed field gradients, coupled to 5-mm triple resonance cryogenic inverse probe (^{1}H, ^{13}C, ^{15}N) operating at 600 MHz. The experimental conditions were as follows: 1.5-s relaxation delay, excitation pulse 7.75 μs wide, 12 ppm spectral window, 64 Kbytes data points, 256 transients per signal (approximately 30 min of acquisition),

and water pulse saturation 1.5 s wide. Most of the water was removed by the lyophilization process, but standard pulse sequence coupled with selective saturation of residual water, PRESAT (John C. Lindon *et al.* 2007), was applied to remove the residual water content signal from the spectrum. The PRESAT method could suppress from 80 to 90% of the residual water signal, which is located at 4.8 ppm. A weighted Fourier Transform with a line broadening of 0.3 Hz was applied to the spectra, followed by phase adjustment and baseline correction through spline curves. The width at half height (LWHH) of the DSS spectral line was used to determine the resolution of measurements that varied from 0.5 to 0.8 Hz. Additionally, the signal to noise ratio (SNR) was used to determine the level of uncertainty of our measurements. For each spectral line obtained, the respective SNR varied from 137 to 3670, an acceptable parameter. On average, the SNR was 998 ± 630.

Normalization of results and statistical analysis Two methods for the normalization of ^{1}H-MRS spectra were applied (Martins-Bach *et al.* 2012; Bacchi *et al.* 2014). First, a chemical shift scale was performed. The DSS shift was adjusted to 0 ppm, and its area was employed to normalize the vertical scale by line shape fitting. Thereby, issues regarding the increase of the resonance spectrometer gain and alterations in the sample's pH that could shift the high-resolution lines were prevented. Then, the total area of each spectrum, calculated between 0.7 to 10.8 ppm, removing noisy ranges and water signal, was used dividing their respective intensities by the corresponding total area. These procedures circumvented the result dependence of the absolute number of resonant protons on the lyophilized sample, corresponding to a mass, volume, or number of cells. A third data normalization applied in MVA consisted of taking each corresponding variable to the 19 area values found in the spectra, ascribed to metabolites, mean centered, and divided by their standard deviation. The normalized "levels" used in the statistical analysis were better obtained either by numerical integration (3 chemical shift intervals) or fitting process (16 multiplet structures), resulting in a total of 19 levels ascribed to 22 metabolites (excluding the DSS signal) (Table 1).

MVA techniques, such as principal components analysis (PCA) and partial least squares-discriminant analysis (PLS-DA), provided an essential approach for rapid interpretation of the information-rich spectral datasets and also to infer about the biological processes (Madsen *et al.* 2010; Worley and Powers 2013). In this sense, PLS-DA, a supervised MVA method to sharpen the separation between groups of observations, was chosen to verify any slight clustering tendencies of samples, which could point differences in metabolic characteristics of the investigated lineages. In PLS-DA, groups of similar samples could be observed in a bi-dimensional plane, while the possible outliers ("chemical signatures"), responsible for grouping samples, were included as variable of importance in projection (VIP scores) (Xia and Wishart 2016).

Table 1. ^{1}H-MRS chemical shift assignments obtained spectral analysis of culture media

Metabolites	Synonyms	Chemical shifts (ppm)
4,4-dimethyl-4-silapentane-1-sulfonic acid	DSS (-CH_3-)$_3$	0
Leucine; isoleucine; valine	Ileu; Leu; Val	1.05–0.80
3-Hydroxybutyrate	3-HBA	1.18
Threonine	Thr	1.25
Lactate	Lac	4.10
Alanine	Ala	1.35
Lysine, arginine	Lys, Arg	1.90–1.55
Pyroglutamate	Pyro	4.19–4.14
Acetate	AcOH	1.90
Acetone	Acetone	2.22
Methionine	Met	2.11
α-glucose	α-GLC	5.20
β-glucose	β-GLC	4.60
Tyrosine	Tyr	7.15
Phenylalanine	Phe	7.40
Histidine	His	8.02
Histamine	HSM	8.03
τ-Methylhistidine	3-MHis	6.98
Formate	Add-F	8.46
Niacinamide	NAM	8.93

Short names (synonyms) in agreement with the Human Metabolome Database (HMDB)

MVA was performed by the SIMCA-P software (Umetrics™, trial license, Malmö, Sweden) and MetaboAnalyst (Xia and Wishart 2016), using a unit scaling option that rescales different variables to make them comparable and provides accurate identification of outlier metabolites. By the PLS-DA method, R^2Y and Q^2 parameters were obtained to indicate the accuracy of variable variation and the predictability of the variable (estimated by cross-validation), respectively. These parameters evaluated the assertiveness of generated results (Xia and Wishart 2016).

Despite the ability of the multivariate method to identify clustering tendencies, the variables (molecules or simply metabolites) were tested according to their respective statistical significance with univariate methods, such as *t* test or ANOVA (Massad, de Menezes, Silveira, & Ortega, 2004; Xia and Wishart 2016). The significance level was set as 0.05 to analyze differences between the metabolites pointed by MVA. All the univariate analyses were performed in Minitab Statistical Software (Minitab Inc., institutional license, State College, PA).

Results

The WT and KO-CSRP3 CMs could not be distinguished by their in vitro morphology. Figure 2 shows the aspect of both

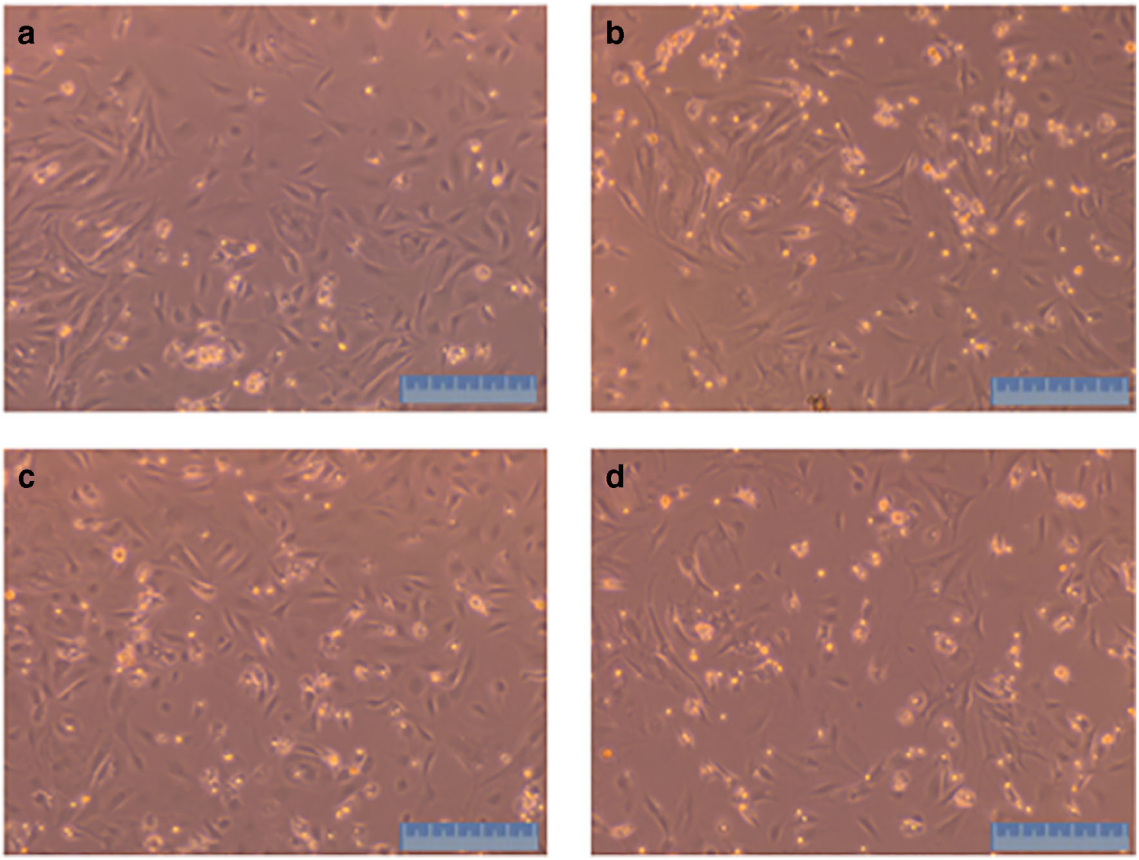

FIGURE 2. Morphological aspects of the effect of isoproterenol upon WT and KO-CSRP3 CMs at 96-h culture. (*a*) Untreated WT (basal condition), (*b*) WT under ISO stimulation, (*c*) KO-CSRP3 at basal condition, (*d*) KO-CSRP3 under ISO stimulation. Photomicroscopies obtained with × 40 magnification in a Leica MC170HD, *scale bar* = 50 μm.

CMs' lineages before and after the administration of isoproterenol. It demonstrates the absence of cytotoxicity and observable changes in the morphology of CMs after ISO stimulation in the assayed conditions. Indeed, ISO did not induce an expressive cellular death, and the cells continued beating after the 24-h exposure. The effects of isoproterenol upon the observed beating frequencies were confirmed as the control parameter of the experimental conditions. It was about a 60% increase for the WT and a 50% increase for the KO-CSRP3 CMs.

The high-resolution resonance lines (singlet, doublet, triplet, quartet, or multiplet structures) were assigned after testing each related component from the DMEM:M199 mixture in the samples of the study, including those without cells. In addition to the media components, metabolites that may be produced by cells were also successfully identified in the spectra. Table 1 summarizes these metabolites, and Fig. 3 shows a typical spectrum of the culture media. Chemical shifts identified corresponding metabolites in the reference spectra (Ellinger *et al.* 2013; Wishart *et al.* 2013; Pereira *et al.* 2014). Metabolite levels were calculated by the line shape areas fitting or by numerical integration.

The generated PLS-DA scores were analyzed using up to four components in the 2D score plot. Only the evident clustering tendency was selected (generally observed at the first two or three components) (Xia and Wishart 2016). PLS-DA identified metabolic differences between the WT and KO-CSRP3 CMs, at either basal or ISO-stimulated conditions, considering the reference values obtained for the medium without cells samples. Figure 4 presents PLS-DA score plots and summarizes the main results obtained for basal (Fig. 4*a*) and ISO-stimulated (Fig. 4*b*) sample comparisons. These results provided insights regarding the consumed and produced metabolites during the media incubation with and without the cells.

The R^2Y and Q^2 were employed to estimate the need for further detailed analysis. Figure 4*a* displays a lower Q^2 value (~ 12%), despite a reasonably high R^2Y value (~ 60%). On the other hand, reasonable R^2Y and Q^2 values were simultaneously displayed in Fig. 4*b*, evidencing that ISO exposure increased metabolic differences between WT and KO-CSRP3 CMs. The outliers, also known as fingerprints (J C Lindon *et al.* 2006; Madsen *et al.* 2010; Martins-Bach *et al.* 2012; Bacchi *et al.* 2014), were assessed in MVA by VIP scores in a list of values organized in descending order. Assuming a minimum threshold of 1 (Xia and Wishart 2016), the peak areas of the ^{1}H resonance spectra components identified with the higher VIP scores were tested by ANOVA coupled with

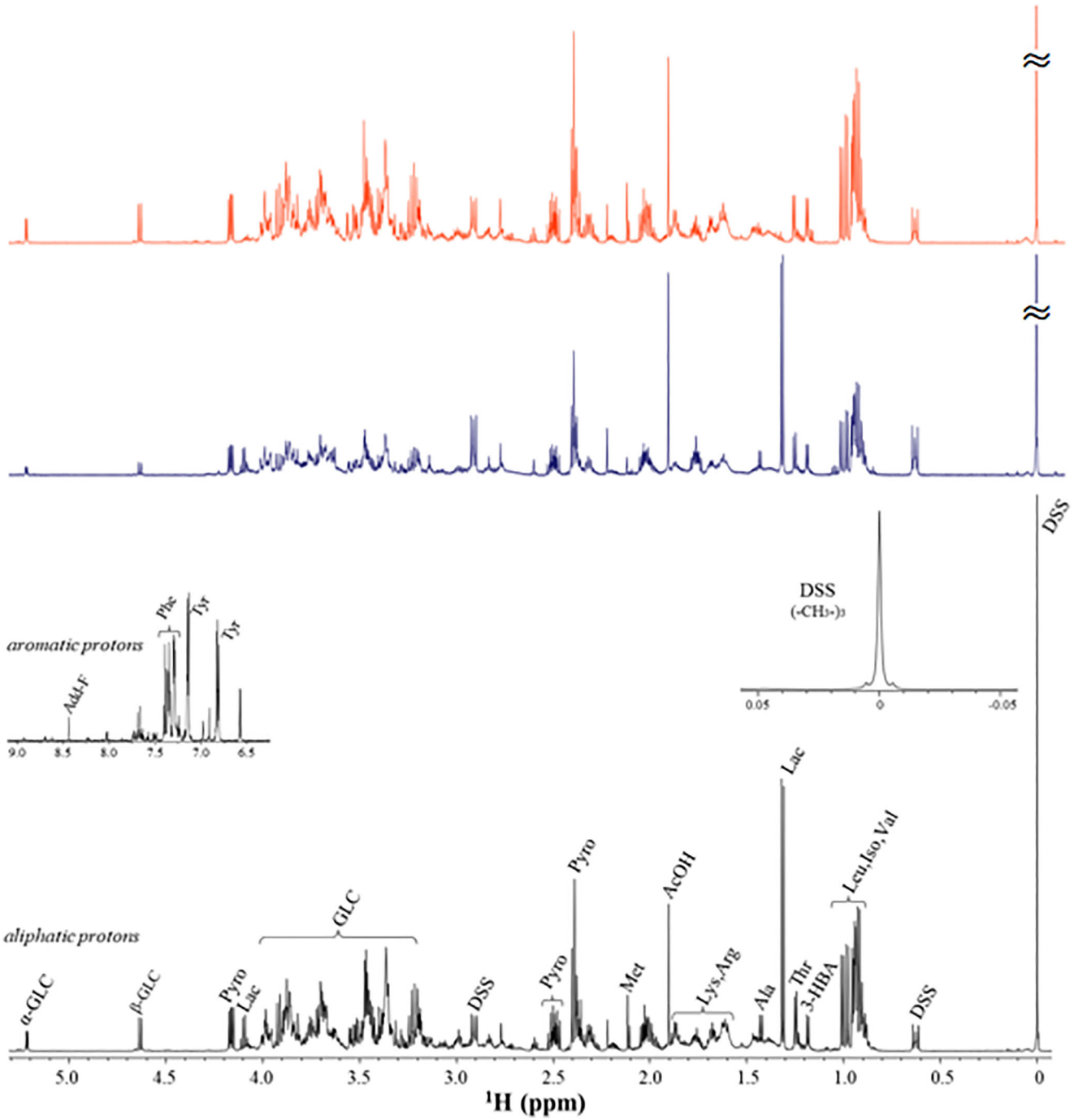

FIGURE 3. Representative ^{1}H high-resolution NMR spectra of unconditioned control (*red*), WT-conditioned (*blue*), and KO-CSRP3-conditioned (*black*) media samples. Peak corresponding metabolites as identified by their short names: acetate (AcOH), alanine (Ala), arginine (Arg), glucose (GLC), formate (Add-F), 3-hydroxybutyrate (3-HBA), isoleucine (Iso), lactate (Lac), leucine (Leu), lysine (Lys), methionine (Met), phenylalanine (Phe), pyroglutamate (Pyro), threonine (Thr), tyrosine (Tyr), and valine (Val). Chemical shift and intensity standard: 4,4-dimethyl-4-silapentane-1-sulfonic acid (DSS). Experimental conditions were as follows: 600 MHz (^{1}H), 25°C, 1.5 s relaxation delay, 7.75 μs excitation pulse, 12 ppm spectral window, 64 Kbytes data points, 256 transients per signal, and 1.5 s water pulse saturation.

Fisher's pairing (Massad *et al.* 2004; Heckler 2005) to differentiate among the metabolite levels associated to the control, WT, and KO-CSRP3 samples in each experimental condition. Normalized concentrations of the identified metabolites are shown in Table 2.

Among the commercially available culture media components, histidine, leucine, isoleucine, valine, lysine, methionine, phenylalanine, threonine, tyrosine, α-glucose, β-glucose, alanine, and niacinamide were identified in this study. Conversely, glycine, arginine, cysteine, glutamine, glutamate,

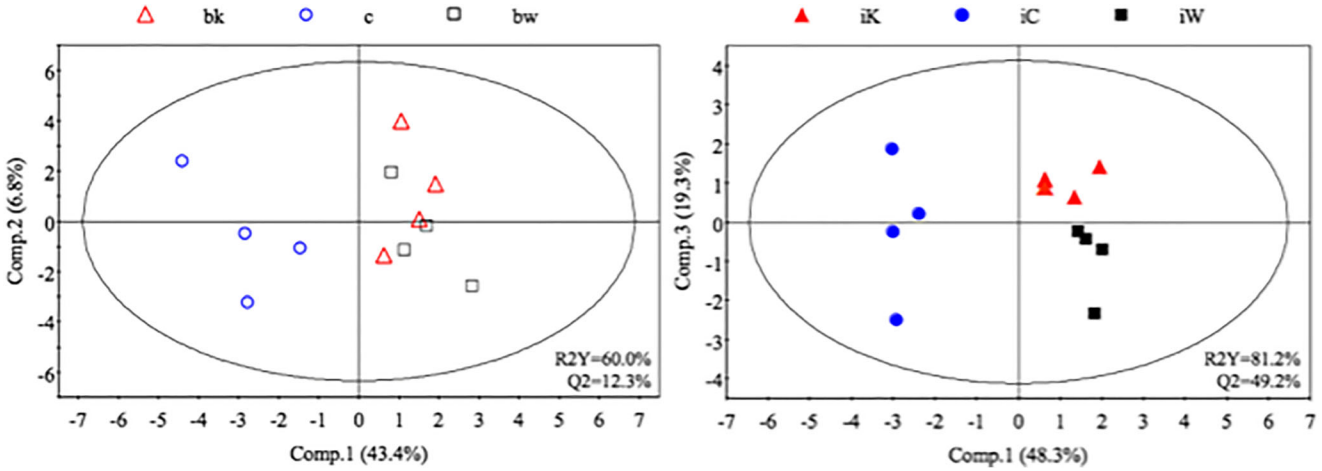

Figure 4. Partial least square discriminant analysis (2D scores plot) obtained from comparisons of culture media at basal (*open symbols, left panel*) and ISO-stimulated (*closed symbols, right panel*). *Squares* are displayed for WT, *triangle* for KO-CSRP3, and *circles* for control groups ($n = 4$). The percentage of explained data variance by each component is shown in the respective axis inside brackets (%). The obtained parameters R^2Y (goodness of fit), Q^2 (predictability), and 95% confidence region (tolerance ellipses as described in Xia and Wishart 2016) for each condition are also shown.

serine, tryptophan, myo-inositol, aspartate, cysteine, hydroxyproline, proline, hydroxycholine, folic acid, riboflavin, thymine, uracil, xanthine, and nicotinamide were not detectable in the spectra of the media samples, because of their concentrations below the limits of detection of the resonance spectrometer (< 100 μM) (Griffin and Shockcor 2004). Furthermore, the inherent low accuracy of resonance spectrometer combined with intense spectral overlapping of signal impaired the proper identification of all the high-resolution lines in spectra. Thus, these high-resolution lines were excluded from the analysis to avoid misinterpretation. The presence of acetate, acetone, 3-hydroxybutyrate, pyroglutamate, lactate, τ-methylhistidine, and formate in culture medium derived from cell metabolism and then were taken as reports of the CMs' metabolic activity, (Madhu *et al.* 2015).

MVA analysis showed a clear separation for the results of the media incubated without cells (upper and bottom left in scores plot) and with cells (upper and bottom right in scores plot of Fig. 4 *a* and *b*). It demonstrates that metabolomics

Table 2. Statistical data analysis of the MVA-pointed metabolites

Metabolite	Basal (mean ± sd; ANOVA Fisher*)			ISO (mean ± sd; ANOVA Fisher**)			ISO effect (*t* test *p* values)		CSRP3 phenotype (*t* test *p* values)	
	bw	bk	c	iW	iK	iC	WT	CSRP3	Basal	ISO
3-HBA	0.93 ± 0.10 *A*	0.97 ± 0.10 *A*	0.87 ± 0.45 *A*	1.06 ± 0.08 *A*	1.10 ± 0.11 *A*	0.76 ± 0.09 *B*	0.90 *iW = bw*	0.14 *iK = bk*	0.64 *bk = bw*	0.63 *iK = iW*
Thr	1.31 ± 0.18 *A*	1.19 ± 0.06 *A*	0.91 ± 0.11 *B*	1.33 ± 010 *A*	1.21 ± 0.09 *A*	0.94 ± 0.04 *B*	0.91 *iW = bw*	0.66 *iK = bk*	0.24 *bk = bw*	0.13 *iK = iW*
Ala	0.61 ± 0.07 *A*	0.60 ± 0.03 *A*	0.21 ± 0.04 *B*	0.66 ± 0.03 *A*	0.72 ± 0.05 *A*	0.24 ± 0.02 *B*	0.19 *iW = bw*	0.01 *iK > bk*	0.78 *bk = bw*	0.11 *iK = iW*
Lac	3.15 ± 0.51 *A*	2.63 ± 0.16 *B*	0.20 ± 0.09 *C*	3.65 ± 0.44 *A*	3.05 ± 0.27 *B*	0.16 ± 0.05 *C*	0.19 *iW = bw*	0.04 *iK > bk*	0.10 *bk = bw*	0.06 *iK = iW*
Tyr	0.94 ± 0.17 *A*	0.96 ± 0.11 *A*	1.42 ± 0.63 *A*	0.86 ± 0.31 *B*	1.65 ± 0.72 *A*	1.11 ± 0.12 *AB*	0.64 *iW = bw*	0.11 *iK = bk*	0.86 *bk = bw*	0.09 *iK = iW*

The comparisons of mean values were performed by ANOVA followed by Fisher's pairing for the comparisons among WT, KO-CSRP3, and control media values at basal or ISO-stimulated conditions or by the Student *t* test and for the comparisons of the basal vs. ISO-stimulated conditions, same cell type, or of the WT vs. KO-CSRP3, same experimental condition. The different letters inserted below the mean ± standard deviation values indicate the statistical differences identified by Fisher's test. All the comparisons considered the 95% confidence level. Numerical values of the normalized areas with respective standard deviations, *p* values, and post hoc analysis results are shown

*$p_{3\text{-HBA}} = 0.89$; $p_{Thr} = 0.01$; $p_{Ala} < 0.01$; $p_{Lac} < 0.01$; $p_{Tyr} = 0.19$

**$p_{3\text{-HBA}} < 0.01$; $p_{Thr} < 0.01$; $p_{Ala} < 0.01$; $p_{Lac} < 0.01$; $p_{Tyr} = 0.09$

could identify the main consumed, produced, or degraded metabolites/components in both CMs' lineages. Despite the group behavior similarity indicated by the partial overlap of WT ("bw") and KO-CSRP3 ("bk") points at basal condition (Fig. 4*a*), a clear separation tendency was detected for "iW" (points in bottom right of the panel) and "iK" (points in the upper right of the panel) in ISO-stimulated condition (Fig. 4*b*). These results demonstrated that metabolomic analysis of culture medium detected isoproterenol-stimulated changes in CMs' metabolism. ANOVA results confirmed higher alanine, lactate, and threonine levels at the CMs' medium than in cell-free medium. Despite alanine and threonine were already present in culture medium before incubation, cellular processes modified its concentrations by consumption, production, or both. Differently, lactate was completely produced by cells. Lactate concentrations could distinguish among the control, WT, KO-CSRP3 groups. ANOVA results are shown in Table 2.

Discussion

Global metabolic differences between control and genetically modified neonatal cardiomyocytes were investigated by ^{1}H-MRS-based metabolomics. As pulsating cells, high-energy amounts are necessary to meet CMs' requirements. The main energy sources for beating CMs are fatty acid oxidation, ketogenic, and glucogenic metabolism (Aliu *et al.* 2018; Nalbandian and Takeda 2016). Besides a convenient energy source, in vitro CMs require essential biochemical substrates, inorganic salts, and pH buffers that must be provided by culture media. The culture medium environment provides the whole set of essential compounds for proper cellular metabolism (Mohmad-Saberi *et al.* 2013). In this context, metabolomics proved to be a suitable tool to study the media components consumed or produced by WT and KO-CSRP3 cells, at basal and ISO-stimulated conditions.

The identification and measurement of individual compounds occurring in such complex mixtures are challenging, and an incomplete analysis may impair metabolomic profiling. Nevertheless, an interesting advantage is observed when considering that the culture medium can be collected at any time, allowing kinetic studies of drug effects through probing and even targeting metabolic components, consumed or secreted by cells into the culture media (Kostidis 2018).

The present study has some limitations that must be addressed. The ^{1}H-MRS is fundamentally a sensitivity-limited technique, especially when compared with mass spectrometer-based techniques. However, it is a non-destructive and much more robust technique (Emwas 2015). The alternative strategy to perform metabolomics analysis in the culture media has been successfully described in the literature (Pereira *et al.* 2014; Chaudhari *et al.* 2017).

Indeed, this approach has provided important insights into the analysis of the CSRP3 genetic polymorphism or mutations. Csrp3 deficiency is considered phenotypically undetectable in the neonatal period of life. Our results demonstrated differences among WT- and Csrp3-deficient cell-conditioned media. Lactate levels were approximately 20% higher in WT cells when compared with KO-CSRP3, at both basal and ISO-stimulated states. The acceleration of energetic metabolism by isoproterenol stimulated lactate production in both lineages. In terms of absolute values, when ISO-stimulated, either WT or KO-CSRP3 CMs produced about 16% more lactate, respective to their untreated counterparts. These results confirm that neonatal WT cells were more prone to perform anaerobic glycolytic metabolism (Triba *et al.* 2010), when compared with KO-CSRP3, independently of isoproterenol stimulation. The inefficient catabolism of KO-CSRP3 lineage could be foreshadowed by the consumption of lactate by the citric acid metabolic pathway. This process might be intermediated by MCP1 and MCP4 monocarboxylate transporter proteins (Nalbandian and Takeda 2016), inducing this metabolite to be consumed as an energetic substrate and reducing the apparent differences between lineages that would otherwise represent the anaerobic lactate production. Ketogenic stress is supported by the increased 3-HBA levels produced by both WT and KO-CSRP3 CMs at ISO-stimulated conditions (Table 2). Fatty acids and ketone bodies are major energy sources for CMs (Klos *et al.* 2019). The ketone body 3-hydroxybutyrate is present in the horse serum supplement for the culture media and is either produced or consumed by the CMs in vitro. WT and KO-CSRP3 were identical with respect to the 3-HBA levels induced by ISO (Table 2).

Regarding Fisher's pairing analysis, no differences were observed between the amino acids measured in the media conditioned by untreated WT or KO-CSRP3 CMs. This situation changed very slightly at ISO-stimulated conditions as reflected by tyrosine levels. Tyrosine is an aromatic amino acid used in ketogenic and glucogenic cellular metabolism. In ketogenic metabolism, tyrosine is converted into acetoacetate, which generates acetyl-CoA for catabolism through lipid degradation routes. In glucogenic metabolism, fumarate is produced from tyrosine and further converted to glucose molecules (Aliu *et al.* 2018). The results suggest that WT CMs effectively use ketogenic and anaerobic metabolism, while higher tyrosine levels and the dissociation of tyrosine levels between WT and KO-CSRP3 CMs implied a higher catabolism of protein-derived substrates by KO-CSRP3 CMs (Table 2).

Present results confirm previously published data from Triba's NMR experiments with intact B16-F10 melanoma cells (Triba *et al.* 2010). They observed that the decreases of alanine and lactate levels were well related, highlighting the role of pyruvate transamination route in the determination of this effect. Considering the reversibility of transamination

reactions, it can be supposed that the alanine increases identified in the spectra could indirectly result from the increased anaerobic lactate production.

High extracellular levels of lactate and alanine, in association with increased 3-HBA production, represent the observed neonate CMs' ketogenic metabolism profile. When the neonate KO-CSRP3 CMs are compared with their WT counterparts, the deficient ketogenic switch was at first revealed by the inability of the KO-CSRP3 CMs to deal with the increased energy requirements imposed by ISO stimulation. Then, it was possible to disclose the KO-CSRP3 CMs' lower ability to use ketone bodies and lactate as an alternative energy source. The very initial signs of the metabolic drift imposed by Csrp3 deficiency may be the increased protein degradation suggested by the statistical differences between basal and ISO-stimulated (increased) lactate and alanine levels that were not verified within the WT CMs.

Conclusions

Our results showed the potential of ^{1}H-MRS-based metabolomics as an exploratory approach to early distinguish biochemical characteristics of two CMs' lineages (WT and KO-CSRP3). By analyzing the in vitro culture media, it was possible to evaluate isoproterenol capacity to increase cell energy requirements and boost metabolic differences between CMs' lineages in aerobic conditions. Particularly, lactate, alanine, threonine, 3-hydroxybutyrate, and tyrosine were considered as classificatory outliers (fingerprints) and discussed in a biochemical perspective. High lactate levels are usually produced by cultured CMs, once heart beating cells rely on aerobic and anaerobic metabolism. ISO-stimulated conditions imply stressing the anaerobic component. Threonine (precursor of acetyl-CoA), 3-hydroxybutyrate (ketone body produced from acetyl-CoA), and tyrosine (aromatic amino acid used in the ketogenic and glucogenic process of cells) levels changed differently, and all these molecules could be directly linked to ketogenesis. The global metabolic response to ISO was different between KO-CSRP3 and WT lineages of neonatal CMs. The KO-CSRP3 CMs were unable in responding as efficiently as WT CMs. Early detection of metabolic markers of the proteasomal overload opens new possibilities for further studies about the metabolic imbalance of CSRP3 mutations and associated cardiomyopathies. In spite of further studies being necessary to elucidate the complex metabolic effects of Csrp3 defects, not only future advances of tissue engineering for regenerative medicine but also sports technologies and several medical specialties would benefit from additional results on CSRP3 coordination of glucose homeostasis and trophic responses of the heart.

Acknowledgments The authors would like to acknowledge the São Paulo Research Foundation (FAPESP) (grants 2011/19678-1; 2013/17368-0; 2014/22102-2; 2014/21646-9; 2018/20910-5) and Medical Sciences Graduate Program-CAPES/PROEX for financial support; LNBio-CNPEM (20992) for providing spectrometer and facilities; Laboratory of Genetics and Molecular Cardiology, Heart Institute (InCor) - University of Sao Paulo School of Medicine for providing cells and scientific assistance; and National Institute of Science and Technology Complex Fluids (INCT-FCX) for daily financial aid.

Authors' contributions ACB and VB equally contributed to cell experiments. ACB contributed with sample preparation, NMR experiments, data processing, statistical analysis, and biological interpretations and drafted the manuscript. LFG critically revised the manuscript. JAS, IVB, VB, and AMA contributed to the design of the research and cell experimental setup. All authors agree to be fully accountable for ensuring the integrity and accuracy of the work and read and approved the final manuscript.

Compliance with ethical standards

Conflicts of interest The authors declare that they have no conflict of interest.

Ethics approval Approval was obtained from the institutional review board from the University of Sao Paulo, School of Medicine, Brazil (#340/12).

References

Aliu E, Kanungo S, Arnold GL (2018) Amino acid disorders. Ann Transl Med 6(24):471–471. https://doi.org/10.21037/atm.2018.12.12

Arber S, Hunter JJ, Ross J, Hongo M, Sansig G, Borg J et al (1997) MLP-deficient mice exhibit a disruption of cardiac cytoarchitectural organization, dilated cardiomyopathy, and heart failure. Cell 88(3):393–403. Retrieved from https://doi.org/10.1186/2193-1801-3-470

Bacchi PS, Bloise AC, Bustos SO, Zimmermann L, Chammas R, Rabbani SR (2014) Metabolism under hypoxia in Tm1 murine melanoma cells is affected by the presence of galectin-3, a metabolomics approach. SpringerPlus 3:470

Boateng SY, Senyo SE, Qi L, Goldspink PH, Russell B (2009) Myocyte remodeling in response to hypertrophic stimuli requires nucleocytoplasmic shuttling of muscle LIM protein. J Mol Cell Cardiol 47(4):426–435. https://doi.org/10.1016/j.yjmcc.2009.04.006

Campos LCG, Ribeiro-Silva JC, Menegon AS, Barauna VG, Miyakawa AA, Krieger JE (2018) Cyclic stretch-induced Crp3 sensitizes vascular smooth muscle cells to apoptosis during vein arterialization remodeling. Clin Sci 132(4):449–459. https://doi.org/10.1042/cs20171601

Chaudhari U, Ellis JK, Wagh V, Nemade H, Hescheler J, Keun HC, Sachinidis A (2017) Metabolite signatures of doxorubicin induced toxicity in human induced pluripotent stem cell-derived cardiomyocytes. Amino Acids 49(12):1955–1963. https://doi.org/10.1007/s00726-017-2419-0

Ehsan M, Kelly M, Hooper C, Yavari A, Beglov J, Bellahcene M et al (2018) Mutant muscle LIM protein C58G causes cardiomyopathy through protein depletion. J Mol Cell Cardiol 121:287–296. https://doi.org/10.1016/j.yjmcc.2018.07.248

Ellinger JJ, Chylla RA, Ulrich EL, Markley JL (2013) Databases and software for NMR-based metabolomics. Curr Metabolomics 1(1):28–40. https://doi.org/10.2174/2213235x11301010028

Emwas AHM (2015) The strengths and weaknesses of NMR spectroscopy and mass spectrometry with particular focus on metabolomics research. Methods Mol Biol 1277:161–193. https://doi.org/10.1007/978-1-4939-2377-9_13

Finckenberg P, Mervaala E (2010) Novel regulators and drug targets of cardiac hypertrophy. J Hypertens 28(Suppl 1):S33–S38. https://doi.org/10.1097/01.hjh.0000388492.73954.0b

Geier C, Perrot A, Özcelik C, Binner P, Counsell D, Hoffmann K et al (2003) Mutations in the human muscle LIM protein gene in families with hypertrophic cardiomyopathy. Circulation 107(10):1390–1395. https://doi.org/10.1161/01.CIR.0000056522.82563.5F

Griffin JL, Shockcor JP (2004) Metabolic profiles of cancer cells. Nat Rev Cancer 4(7):551

Heckler CE (2005) Applied multivariate statistical analysis: applied multivariate statistical analysis. Technometrics 47(4):517–517. https://doi.org/10.1198/tech.2005.s319

Hernandez-Carretero A, Weber N, LaBarge SA, Peterka V, Doan NYT, Schenk S, Osborn O (2018) Cysteine- and glycine-rich protein 3 regulates glucose homeostasis in skeletal muscle. Am J Physiol-Endocrinol Metab 315(2):E267–E278. https://doi.org/10.1152/ajpendo.00435.2017

Jensen L, Neri E, Bassaneze V, De Almeida Oliveira NC, Dariolli R, Turaça LT, … Krieger JE (2018) Integrated molecular, biochemical, and physiological assessment unravels key extraction method mediated influences on rat neonatal cardiomyocytes. J Cell Physiol 233(7):5420–5430. https://doi.org/10.1002/jcp.26380

Kaddurah-Daouk R, Kristal BS, Weinshilboum RM (2008) Metabolomics: a global biochemical approach to drug response and disease. Annu Rev Pharmacol Toxicol 48:653–683. https://doi.org/10.1146/annurev.pharmtox.48.113006.094715

Klos M, Morgenstern S, Hicks K, Suresh S, Devaney EJ (2019) The effects of the ketone body β-hydroxybutyrate on isolated rat ventricular myocyte excitation-contraction coupling. Arch Biochem Biophys 662:143–150. https://doi.org/10.1016/J.ABB.2018.11.027

Kostidis S (2018) Quantitative analysis of central energy metabolism in cell culture samples. Methods Mol Biol 1730:329–342. https://doi.org/10.1007/978-1-4939-7592-1_25

Lange S, Gehmlich K, Lun AS, Blondelle J, Hooper C, Dalton ND et al (2016) MLP and CARP are linked to chronic PKCα signaling in dilated cardiomyopathy. Nat Commun 7(1):12120. https://doi.org/10.1038/ncomms12120

Li R, Yan G, Zhang Q, Jiang Y, Sun H, Hu Y et al (2013) miR-145 inhibits isoproterenol-induced cardiomyocyte hypertrophy by targeting the expression and localization of GATA6. FEBS Lett 587:1754–1761

Li X, Lu WJ, Li Y, Wu F, Bai R, Ma S et al (2019) MLP-deficient human pluripotent stem cell derived cardiomyocytes develop hypertrophic cardiomyopathy and heart failure phenotypes due to abnormal calcium handling. Cell Death Dis 10(8). https://doi.org/10.1038/s41419-019-1826-4

Lindon JC, Holmes E, Nicholson JK (2006) Metabonomics techniques and applications to pharmaceutical research & development. Pharm Res 23(6):1075–1088. https://doi.org/10.1007/s11095-006-0025-z

Lindon JC, Nicholson JK, Holmes E (2007) The Handbook of Metabonomics and Metabolomics. In: The Handbook of Metabonomics and Metabolomics. https://doi.org/10.1016/B978-0-444-52841-4.X5000-0

Madhu B, Dadulescu M, Griffiths J (2015) Artifacts in 1H NMR-based metabolomic studies on cell cultures. MAGMA 28(2):161–171. https://doi.org/10.1007/s10334-014-0458-z

Madsen R, Lundstedt T, Trygg J (2010) Chemometrics in metabolomics - a review in human disease diagnosis. Anal Chim Acta 659:23–33

Mandenius C-F, Steel D, Noor F, Meyer T, Heinzle E, Asp J et al (2011) Cardiotoxicity testing using pluripotent stem cell-derived human cardiomyocytes and state-of-the-art bioanalytics: a review. J Appl Toxicol 31(3):191–205. https://doi.org/10.1002/jat.1663

Martínez MS, García A, Luzardo E, Chávez-Castillo M, Olivar LC, Salazar J et al (2017) Energetic metabolism in cardiomyocytes: molecular basis of heart ischemia and arrhythmogenesis. Vessel Plus 1(12). https://doi.org/10.20517/2574-1209.2017.34

Martins-Bach AB, Bloise AC, Vainzof M, Rabbani SR (2012) Metabolic profile of dystrophic mdx mouse muscles analyzed with in vitro magnetic resonance spectroscopy (MRS). Magn Reson Imaging 30:1167–1176

Massad E, de Menezes RX, Silveira PSP, Ortega NRS (2004) Métodos Quantitativos em Medicina. Manole

Mohmad-Saberi SE, Hashim YZH-Y, Mel M, Amid A, Ahmad-Raus R, Packeer-Mohamed V (2013) Metabolomics profiling of extracellular metabolites in CHO-K1 cells cultured in different types of growth media. Cytotechnology 65(4):577–586. https://doi.org/10.1007/s10616-012-9508-4

Nalbandian M, Takeda M (2016) Lactate as a signaling molecule that regulates exercise-induced adaptations. Biology 5(4):38. https://doi.org/10.3390/biology5040038

Nicholson JK (2010) 2020 visions. Nature 463(7277):26–32. https://doi.org/10.1038/463026a

Pereira T, Ivanova G, Caseiro AR, Barbosa P, Bártolo PJ, Santos JD et al (2014) MSCs conditioned media and umbilical cord blood plasma metabolomics and composition. PLoS ONE 9(11):e113769. https://doi.org/10.1371/journal.pone.0113769

Saborano R, Eraslan Z, Roberts J, Khanim FL, Lalor PF, Reed MAC, Günther UL (2019) A framework for tracer-based metabolism in mammalian cells by NMR. Sci Rep 9(1). https://doi.org/10.1038/s41598-018-37525-3

Triba MN, Starzec A, Bouchemal N, Guenin E, Perret GY, Le Moyec L (2010) Metabolomic profiling with NMR discriminates between biphosphonate and doxorubicin effects on B16 melanoma cells. NMR Biomed 23:1009–1016. https://doi.org/10.1002/nbm.1516

Wishart DS, Jewison T, Guo AC, Wilson M, Knox C (2013) HMDB 3.0 - The human metabolome database in 2013. Nucleic Acids Res 41:801–807

Worley B, Powers R (2013) Multivariate analysis in metabolomics. Curr Metabolomics 1(1):92–107. https://doi.org/10.2174/221323X11301010092

Xia J, Wishart DS (2016) Using MetaboAnalyst 3.0 for comprehensive metabolomics data analysis. Curr Protoc Bioinformatics 55:14.10.1–14.10.91

Zhang Y, Sekar RB, McCulloch AD, Tung L (2008) Cell cultures as models of cardiac mechanoelectrical feedback. Prog Biophys Mol 97:367–382